IOP Publishing Inverse Problems

Inverse Problems **34** (2018) 125003 (23pp) https://doi.org/10.1088/1361-6420/aae04d

A regularization method based on level sets and augmented Lagrangian for parameter identification problems with piecewise constant solutions

J P Agnelli[1], A De Cezaro[2] and A Leitão[3]

[1] FaMAF-CIEM (CONICET), Universidad Nacional de Córdoba, Medina Allende S/N 5000, Córdoba, Argentina
[2] Institute of Mathematics Statistics and Physics, Federal University of Rio Grande, Av. Italia km 8, 96201-900 Rio Grande, Brazil
[3] Department of Mathematics, Federal University of St. Catarina, PO Box 476, 88040-900 Florianópolis, Brazil

E-mail: agnelli@famaf.unc.edu.ar, decezaromtm@gmail.com and acgleitao@gmail.com

Received 17 March 2018, revised 3 September 2018
Accepted for publication 11 September 2018
Published 1 October 2018

Abstract

We propose and analyse a regularization method for parameter identification problems modeled by ill-posed nonlinear operator equations, where the parameter to be identified is a piecewise constant function taking known values.

Following (De Cezaro *et al* 2013 *Inverse Problems* **29** 015003), a piecewise constant level set approach is used to represent the unknown parameter, and a corresponding Tikhonov functional is defined on an appropriated space of level set functions. Additionally, a suitable constraint is enforced, resulting that minimizers of our Tikhonov functional belong to the set of piecewise constant level set functions. In other words, the original parameter identification problem is rewritten in the form of a constrained optimization problem, which is solved using an augmented Lagrangian method.

We prove the existence of zero duality gaps and the existence of generalized Lagrangian multipliers. Moreover, we extend the analysis in De Cezaro *et al*'s work (2013 *Inverse Problems* **29** 015003), proving convergence and stability of the proposed parameter identification method.

A primal-dual algorithm is proposed to compute approximate solutions of the original inverse problem, and its convergence is proved. Numerical examples are presented: this algorithm is applied to a 2D diffuse optical tomography problem. The numerical results are compared with the ones in

Agnelli *et al* (2017 *ESAIM: COCV* **23** 663–83) demonstrating the effectiveness of this primal-dual algorithm.

Keywords: ill-posed problems, regularization, level-set approach, augmented Lagrangian method

(Some figures may appear in colour only in the online journal)

1. Introduction

In this manuscript we consider the inverse problem of identifying an unknown parameter function $u \in X$, which is assumed to be a piecewise constant function (taking known values) defined on a given bounded domain $\Omega \subset \mathbb{R}^d$, $d = 2, 3$. This parameter function is to be recovered from a given set of data $y \in Y$, with the relation between u and $y \in Y$ being described by the operator equation

$$F(u) \;=\; y\,. \tag{1}$$

Here $F : D(F) \subset X \to Y$ is a possibly nonlinear operator, $X = L_p(\Omega)$ for $1 \leqslant p < d/(d-1)$ and Y is a Banach space. The list of applications fitting this framework is considerable and we refer the reader to [8, 17, 23, 35] and references therein for some relevant examples.

In real life applications, the data in (1) is obtained by indirect measurements of the parameter u. Moreover, the exact data $y \in Y$ is not known in general. Instead, only approximate measured data $y^\delta \in Y$ (corrupted by noise) is available. Here we assume that

$$\|y^\delta - y\|_Y \;\leqslant\; \delta\,, \tag{2}$$

where the level of noise $\delta > 0$ is either known or can be estimated.

The method discussed in this article is designed for solving the operator equation (1), under the *special assumption* that the parameter $u : \Omega \to \mathbb{R}$ is a piecewise constant function taking only two known values, i.e. $u(x) \in \{c^1,\ c^2\}$ a.e. in Ω. With this assumption the inverse problem reduces basically to a shape identification problem.

It is worth mentioning that our method can be extended to the case where the parameter function u takes any finite number of (known) values $\{c^1, \ldots, c^n\}$. The corresponding convergence analysis requires arguments similar to the ones presented here for the Cartesian product topology. However, if the values $\{c^1, c^2\}$ are unknown, our approach no longer applies. For such inverse problems see [13, 14].

Taking into account the above assumption on the solution u, one concludes that there exists an open mensurable set $D_1 \subset\subset \Omega$ such that $u(x) = c^1$, $x \in D_1$, and $u(x) = c^2$, $x \in \Omega \setminus D_1 =: D_2$. Due to this particular structure of the unknown parameter u, it can be represented by means of a piecewise constant level set function $\hat{\phi}$ as follows:

- Define $\hat{\phi} : \Omega \to \mathbb{R}$ by $\phi(x) := i - 1$, $x \in D_i$;
- Define the real functions $\psi_1(t) = 1 - t$, $\psi_2(t) = t$;
- Note that the characteristic functions of D_i satisfy $\chi_{D_i}(x) = \psi_i(\hat{\phi}(x))$, $i = 1, 2$;
- The parameter function u can be represented in the form

$$u \;=\; c^1\psi_1(\hat{\phi}) + c^2\psi_2(\hat{\phi}) \;=:\; P_{pc}(\hat{\phi})\,. \tag{3}$$

The framework used in (3) to represent the solution u of (1) is known in the literature as *piecewise constant level set* (PCLS) approach (see [12, 15, 32, 35] and the references therein). Differently from classical level set approaches (see, e.g. [21, 30]), which are based on smooth

level set functions, here the function $\hat{\phi}$ is assumed to be non-smooth (piecewise constant) [12, 15, 32, 37].

In what follows, the PCLS approach (3) is used as starting point to define a system of operator equations (4) and a corresponding constrained optimization problem (5), which play a key role in the new method proposed in this article for obtaining stable solutions of the inverse problem under consideration.

First we define the (nonlinear) operator $\mathcal{K} : \phi \mapsto \phi(\phi - 1) =: \mathcal{K}(\phi)\,, \quad \phi \in L_4(\Omega)$. Since the level set function $\hat{\phi} \in L_4(\Omega)$ and satisfies $\hat{\phi}(x) := i - 1$, $x \in D_i$, $i = 1, 2$, it follows $\mathcal{K}(\hat{\phi}) = 0$. Reciprocally, if $\mathcal{K}(\phi) = 0$ then $\phi(x) \in \{0, 1\}$, a.e. in Ω (see lemma 2 (ii) below). Consequently, the inverse problem of solving (1), with data satisfying (2), is equivalent to the system of operator equations

$$F(P_{pc}(\phi)) \;=\; y^{\delta}\,, \quad \mathcal{K}(\phi) \;=\; 0. \tag{4}$$

Indeed, if ϕ solves system (4) then, due to the PCLS approach (3), $u := P_{pc}(\phi)$ is a solution of the inverse problem under consideration.

A standard way of obtaining approximate solutions to (4) is to consider the following (regularized) constrained optimization problem

$$\begin{cases} \min \mathcal{F}_{\alpha}(\phi) := \|F(P_{pc}(\phi)) - y^{\delta}\|_Y^2 \;+\; \alpha\mathcal{R}(\phi) \\ \text{s.t.}\;\; \mathcal{K}(\phi) = 0 \end{cases} \tag{5}$$

where $\alpha > 0$ plays the role of a regularization parameter and $\mathcal{R}(\cdot)$ represents the regularization term (see section 2 for detailed definitions). In this manuscript, solutions ϕ_{α}^{δ}, $\alpha > 0$ of (5) are computed using an augmented Lagrangian method. Furthermore, such approach defines a regularization method suitable for the inverse problem discussed in (1) and (2) with piecewise constant solutions (see section 3).

1.1. Review on level set type methods for inverse problems

Level set methods for solving inverse problems were introduced in the seminal paper [34]. Later, during the late 90s and early 2000s, the level set framework was the basis for designing solution methods for ill-posed problems with piecewise constant solutions [7, 21, 30]. Several applications can be found in the literature, among which we mention: image reconstruction [8, 17, 34, 35], inverse potential problem [12, 21], elliptic inverse problems [9, 29, 32] electrical impedance tomography [10, 26, 35], inverse scattering [16, 31], optimal design [8, 35], semiconductors [28], optical diffusion tomography [2] and crack detection [3, 17]. We also refer the reader to the review papers [8, 35] for further applications.

Level set type methods as the one in [34] are iterative methods, where a smooth level set function is used to represent the unknown parameter. The evolution of this function is described by a Hamilton–Jacobi equation, and aims to minimize a quadratic functional of the residual [8, 17, 31].

The so called *standard level set* methods (SLS) for (1) consist in representing the piecewise constant parameter function u by a smooth level set function; the relation between these two functions being described by a discontinuous projection operator (e.g. the Heaviside projector) [9, 30]. Convergence and stability analysis can be found in [21]. On the other hand, problems where two or more piecewise constant parameters (taking only two values) are to be reconstructed, can also be solved by these methods [2].

Multiple level set methods (MSLS) are a variation of the SLS type methods, where several level set functions are used to represent the piecewise constant parameter function u, which is allowed to take more than two distinct constant values [13, 14, 35].

It is worth mentioning the family of *piecewise constant level set* methods (PCLS) [12, 15, 32, 35], where the piecewise constant parameter function u is described by a discontinuous level set function. The relation between these two functions being described by a smooth projection operator (as in (3)). The discontinuity of the level function is enforced by a constraint (as in (4)).

1.2. Remarks on augmented Lagrangian type methods

- Penalty and classical Lagrangian methods are well-known techniques [22, 33] for solving constrained optimization problems as in (5). Moreover, duality theory (existence of Lagrange multipliers) obtained through the classical Lagrangian and its use for constrained convex optimization problems is also well established (see, e.g. [22, 25, 33] and the references therein).
- When the primal problem is not convex, a duality gap (the difference between the optimal primal value and the optimal dual value) may occur when the classical Lagrangian is used [22, 33]. In such cases, it is necessary to search for other kinds of Lagrangian formulations, which are able to provide efficient algorithms for solving broader families of constrained optimization problems including (5) (see, e.g. [5, 33]).
- The augmented Lagrangian approach followed here can be understood as a combination of the penalty function method with the classical Lagrangian multiplier method; and is able to eliminate many disadvantages associated with either method alone (see, e.g. [33]).
- In connection with inverse problems, numerical applications of augmented Lagrangian (coupled with level set methods) can be found in the literature, e.g. in Electrical impedance tomography [35] and in Elliptic inverse problems [9, 32]. Moreover, numerical applications of augmented Lagrangian (without level sets) were used for parameter identification in imaging, e.g. [27, 36].
  In [20], a convergence analysis (with rates) of a non-stationary augmented Lagrangian method for linear inverse problems in Hilbert spaces is derived.
  In [15], an augmented Lagrangian method is coupled with the PCLS method (3) for solving nonlinear parameter identification problems with discontinuous solutions. There, existence of generalized Lagrange multipliers and zero duality gap is proven (from what follows that (5) can be solved as an unconstrained optimization problem for the augmented Lagrangian proposed in [15]).

1.3. Main contributions of this article

- We extend and complete the analysis (both theoretical and numerical) initiated in [15], where PCLS type approaches for solving ill-posed problems are considered in connection with augmented Lagragian methods (see remark 1).
- We follow the PCLS approach used in [15] with a different Tikhonov functional in order to formulate the constrained optimization problem (5) (the constraint and the regularization term used in this paper differ from the ones proposed in [15]).
  For such formulation, we are able to prove existence of a zero duality gap and existence of generalized Lagrangian multipliers, analogue to the results proved in [15].

Additionally, we extend the convergence analysis presented in [15] proving convergence and stability for ϕ_α^δ (solutions of (5)). These results do characterize our solution method as a regularization method in the sense of [18].
– The numerical algorithm discussed in [15] is improved. Here we propose a primal-dual iterative method for computing approximate solutions of (5); convergence of this algorithm is proven (see theorem 7).
– We apply our numerical algorithm to a 2D *diffuse optical tomography* (DOT) benchmark problem [2, 4, 23]. In [2] numerical experiments using SLS were shown for this parameter identification problem; we use here the same numerical setting as in [2] and compare there numerical results with the ones obtained in this article. It is worth mentioning that in [2] a splitting strategy was used in the reconstruction of the unknown pair of parameters (a similar splitting strategy is also used here). However, due to the augmented Lagrangian formulation used here, the number of iterations required for the convergence of our method is much smaller than the one in [2].

1.4. Outline of the paper

In the Introduction we discussed the PCLS approach used here to represent the solution of the inverse problem (1) and (2). Moreover, we derived the constrained optimization problem (5), which is the basis of our solution method. In section 2 we discuss the main assumptions used in this manuscript, and introduce the augmented Lagrangian approach for solving (5). In section 3, we present convergence analysis results. First, the existence of a zero-duality gap and an exact penalty representation for the primal-dual strategy are proved. Then, these properties are employed to show that the proposed solution method is convergent and stable with respect to the noise level in the data. In section 4 a primal-dual algorithm is derived, aiming to compute approximate solutions of (5). A convergence proof is provided. In section 5 several numerical experiments are conducted. Three distinct parameter identification problems related to the DOT problem are solved and the results are compared with the ones obtained in [2]. Section 6 is devoted to final remarks and conclusions. The DOT problem is briefly revised in appendix A, while the algorithm used in the numerical experiments is described in details in appendix B.

2. An augmented Lagrangian method and the PCLS approach

In this section we discuss an augmented Lagrangian type method for solving the constrained optimization problem (5), with the functional $\mathcal{F}_\alpha : L_4(\Omega) \cap \mathtt{BV}(\Omega) \to \mathbb{R}_+$, the operator $\mathcal{K} : L_4(\Omega) \to L_2(\Omega)$ and the penalization functional $\mathcal{R} : L_4(\Omega) \cap \mathtt{BV}(\Omega) \to \mathbb{R}_+$ defined by

$$\mathcal{R}(\phi) \;:=\; \|\phi\|_{L_4}^4 + \beta |P_{pc}(\phi)|_{\mathtt{BV}}\,, \tag{6}$$

where $\beta > 0$ is a scaling factor. It is worth mentioning that the L_4–norm act as a penalization for the level set function on the space $L_4(\Omega)$, whereas the BV-seminorm is well known for penalizing the length of the Hausdorff measure of the boundary of the level sets of $P_{pc}(\phi)$, see [19]. Furthermore, these two terms imply the coercivity of $\mathcal{R}$.

Due to lack of convexity of the Tikhonov functional $\mathcal{F}_\alpha$ classical Lagrange multiplier methods [33] cannot be applied in a straightforward way to solve problem (5), since it is not clear that in general one can prove a zero duality gap property. Following the ideas in [15], we

propose an augmented Lagrangian method based on the abstract convexity framework introduced in [33] to obtain a regularized solution to (5).

We consider the augmented Lagrangian functional $\mathcal{L}_\alpha$, which is formally defined by

$$\mathcal{L}_\alpha(\phi;\lambda,\mu) := \|F(P_{pc}(\phi)) - y^\delta\|_Y^2 + \alpha\mathcal{R}(\phi) + \langle\lambda\,,\mathcal{K}(\phi)\rangle_{L_2(\Omega)} + \mu\|\mathcal{K}(\phi)\|_{L_2(\Omega)}\,, \tag{7}$$

where $\phi \in L_4(\Omega)\cap \mathtt{BV}(\Omega)$, $\lambda \in L_2(\Omega)$ can be interpreted as a 'generalized' Lagrange multiplier and the scalar $\mu > 0$ is a penalty factor that allows one to establish a duality relation for problems of non-convex type (here $\langle\cdot,\cdot\rangle$ denotes the inner product in L_2). This particular augmented Lagrangian functional is known as the sharp Lagrangian [33, chapter 11, section K*].

In the sequel the main assumptions are presented. These are assumed to hold for the remaining of this article.

Main assumptions:

(A1) $\Omega \subseteq \mathbb{R}^d$, $d = \{2, 3\}$, is bounded with boundary $\partial\Omega$ Lipschitz.

(A2) The operator $F : D(F) \subset X = L_p(\Omega) \to Y$ is continuous on $D(F)$ with respect to the L_p-topology, where $1 \leqslant p < d/(d-1)$.

(A3) α, β denote positive parameters and $|c^1 - c^2| \geqslant \hat{c} > 0$.

(A4) There exists $\hat{u} \in \mathtt{BV}(\Omega)\cap L_\infty(\Omega)$ satisfying $F(\hat{u}) = y$. Moreover, there exists a function $\hat{\phi} \in \mathtt{BV}(\Omega)\cap L_4(\Omega)$ such that $P_{pc}(\hat{\phi}) = \hat{u}$ and $\mathcal{K}(\hat{\phi}) = 0$.

In the following definition we introduce some notation and functions related to the augmented Lagrangian approach that are necessary for the forthcoming analysis.

Definition 1. Let $\mathcal{F}_\alpha$ and $\mathcal{K}$ be defined as above.

1. A function ϕ is called admissible if $\phi \in L_4(\Omega)\cap \mathtt{BV}(\Omega)$.
2. $\Gamma : L_4(\Omega) \rightrightarrows L_2(\Omega)$ is the set valued function satisfying $\Gamma(z) := \{\phi \in L_4(\Omega); \mathcal{K}(\phi) = z\}$, for each $z \in L_2(\Omega)$.
3. The indicator function of a set A is defined by $\delta_A(z) := 0$, if $z \in A$ and $\delta_A(z) := +\infty$, otherwise.
4. We define $\widetilde{\mathcal{F}_\alpha}(\phi) := \mathcal{F}_\alpha(\phi)$, if $\phi \in L_4(\Omega)\cap \mathtt{BV}(\Omega)\cap\Gamma(0)$ and $\widetilde{\mathcal{F}_\alpha}(\phi) := +\infty$, otherwise.
5. A dualizing parametrization function for $\widetilde{\mathcal{F}_\alpha}$ is chosen in the following way $f : L_4(\Omega)\times L_2(\Omega) \to \mathbb{R}\cup\{+\infty\}$, with $f(\phi, z) := \mathcal{F}_\alpha(\phi) + \delta_{\Gamma(z)}(\phi)$ if $\phi \in L_4(\Omega)\cap \mathtt{BV}(\Omega)$ and $f(\phi, z) = +\infty$, otherwise. The function f satisfies $f(\phi, 0) = \widetilde{\mathcal{F}_\alpha}(\phi)$, for each $\phi \in L_4(\Omega)$.
6. The perturbation function (of the primal problem) related to this duality parametrization is given by $\theta : L_2(\Omega) \to \mathbb{R}$, where $\theta(z) := \inf_{\phi\in L_4(\Omega)} f(\phi, z)$.
7. The coupling function $\rho : L_2(\Omega)\times L_2(\Omega)\times\mathbb{R}_+ \to \mathbb{R}$ is defined by $\rho(z,\lambda,\mu) := -\langle\lambda, z\rangle - \mu\,\|z\|_{L_2}$.
8. The augmented Lagrangian functional induced by the coupling function ρ reads as
$$\mathcal{L}_\alpha(\phi;\lambda,\mu) = \inf_{z\in L_2(\Omega)}\{f(\phi, z) - \rho(z,\lambda,\mu)\}. \tag{8}$$
9. The dual function $Q : L_2(\Omega)\times\mathbb{R}_+ \to \mathbb{R}$ is defined by $Q(\lambda,\mu) := \inf_{\phi\in L_4(\Omega)} \mathcal{L}_\alpha(\phi;\lambda,\mu)$ and the dual problem is stated as
$$\text{maximize } Q(\lambda,\mu) \quad \text{subject to } (\lambda,\mu) \in L_2(\Omega)\times\mathbb{R}_+.$$

It follows from item 5 of definition 1 that the functional $\mathcal{L}_\alpha$ defined in (7) coincides with the functional in (8) (indeed, the dualizing parameter function f satisfies $f(\phi, z) = +\infty$ whenever $\phi \notin \Gamma(z)$). Moreover, $\mathcal{L}_\alpha(\phi; \lambda, \mu)$ coincides with $\mathcal{F}_\alpha(\phi)$ in (5) whenever $\mathcal{K}(\phi) = 0$.

On the other hand, it follows from item 9 of definition 1 that $Q(\lambda, \mu) = \inf_{z \in L_2(\Omega)}\{\theta(z) - \rho(z, \lambda, \mu)\}$, where θ is the perturbation function.

Now, denoting by $M_p := \inf_{\phi \in L_4(\Omega)} \widetilde{\mathcal{F}_\alpha}(\phi)$ the optimal value of the primal problem, and by $M_d := \sup_{(\lambda,\mu) \in L_2(\Omega) \times \mathbb{R}_+} Q(\lambda, \mu)$ the optimal value of the dual problem. It follows from the definitions of f and ρ the weak duality property for our scheme, i.e.

$$M_d \leqslant M_p\,. \tag{9}$$

We recall that the duality gap is the difference between the values M_p and M_d. In the next section we shall show that our duality scheme satisfies the zero duality gap property ($M_p = M_d$).

Another important concept related to the augmented Lagrangian is the exact penalty representation [5, 33].

Definition 2. A vector $\bar{\lambda} \in L_2(\Omega)$ is said to support an *exact penalty representation* for the problem of minimizing $\widetilde{\mathcal{F}_\alpha}$, if there exists $\bar{\mu} > 0$ such that for any $\mu > \bar{\mu}$

$$\theta(0) = Q(\bar{\lambda}, \mu) \qquad \text{and} \qquad \operatorname{argmin}_\phi \widetilde{\mathcal{F}_\alpha}(\phi) = \operatorname{argmin}_\phi \mathcal{L}_\alpha(\phi; \bar{\lambda}, \mu)\,. \tag{10}$$

Alternatively, such a vector $\bar{\lambda}$ is said to support an exact penalty representation for the problem of minimizing $\mathcal{F}_\alpha$ under the constraint $\mathcal{K}(\phi) = 0$.

3. Convergence analysis

This section is devoted to the analysis of the augmented Lagrangian proposed in (7). We state two main results: (a) existence of zero duality gap and existence of an exact penalty representation for the duality scheme induced by the augmented Lagrangian function (7); (b) well-posednes of the augmented Lagrangian and convergence and stability of approximated solutions, that, in particular, imply that the augmented Lagrangian approach is a regularization method for ill-posed problems.

3.1. Existence of an exact penalty representation

The existence of an exact penalty representation (theorem 1) is the key ingredient to prove the well-posedness, the convergence and stability of approximate solutions given by the augmented Lagrangian (7). The proof of this theorem follows the lines of the proof of [15, theorem 11] (this is due to the fact that the framework established in definition 1 is analogous to the corresponding framework used in [15, section 3]).

Theorem 1. *For any $\alpha > 0$, let $\mathcal{F}_\alpha$ and $\mathcal{K}$ be defined as above.*

(i) There exists $\bar{\lambda} \in L_2(\Omega)$ supporting an exact penalty representation in the sense of definition 2.
(ii) There is no duality gap, i.e. $M_p = M_d$.

Sketch of the proof: Assertion (i): note that the dualizing parametrization function $f(\phi, \cdot)$ is lower semi continuous at $z = 0$, for every $\phi \in L_4(\Omega)$ (see definition 1, item 5). The coupling function $\rho(\cdot, \lambda, \mu)$ is lower semi continuous at $z = 0$. Furthermore, $\rho(z, \lambda, \cdot)$ is monotone

decreasing and satisfies $\rho(0,\lambda,\mu)=0$ (see definition 1, item-6). The perturbation function $\theta(z)$ is lower semi continuous at $z=0$. Moreover, from assumption (A4), it follows that the set of primal solutions is not empty and, consequently, $\theta(0)<+\infty$ (see definition 1, item 6). Finally, arguing as in [15, lemmas 7, 8 and 10], we can conclude the existence of $(\overline{\lambda},\overline{\mu})$ satisfying $\theta(z)\geqslant\theta(0)+\rho(z,\overline{\lambda},\overline{\mu})$, $\forall z\in L_2(\Omega)$.

It now follows from [5, theorem 3.3] that these facts above are equivalent to the assertion (i).

To prove assertion (ii), note that assertion (i) implies

$$M_p=Q(\overline{\lambda},\mu)\leqslant\sup_{(\lambda,\mu)}Q(\lambda,\mu)=M_d.$$

This inequality, together with the weak duality property (9), imply $M_d=M_p$. □

3.2. Convergence and stability

In this subsection, we prove the well-posedness, convergence and stability of approximated solutions given by the (primal) minimizers of the augmented Lagrangian method. Such results imply, in particular, that the proposed solution method is a regularization method [18]. We start with a lemma that contains some essential tools concerning the operators $\mathcal{K}$ and P_{pc} needed to derive the main results of this section.

Lemma 2. *Let $\mathcal{K}$ be the operator defined in section 1 and P_{pc} the operator defined in (3). For $1\leqslant p<d/(d-1)$, the following assertions hold:*

(i) $\mathcal{K}$ is a continuous map from $L_4(\Omega)$ to $L_2(\Omega)$. Additionally, the functional $\|\mathcal{K}(\cdot)\|_{L_1(\Omega)}$, defined in $L_4(\Omega)$, is weakly lower semi-continuous.
(ii) If $\|\mathcal{K}(\phi)\|_{L_2(\Omega)}=0$ for some $\phi\in L_4(\Omega)$, then $\phi(x)\in\{0,1\}$ a.e. in Ω.
(iii) If $\{\phi_k\}$ is a sequence of functions such that $\phi_k\rightharpoonup\bar{\phi}$ in $L_4(\Omega)$ and $\mathcal{K}(\phi_k)=0$ in $L_2(\Omega)$, then $\mathcal{K}(\bar{\phi})=0$ a.e. in Ω.
(iv) For every admissible function ϕ, we have $|P_{pc}(\phi)|_{\mathtt{BV}}\geqslant\hat{c}|\phi|_{\mathtt{BV}}$.
(v) Moreover, if ϕ_k is a sequence of admissible functions converging in $L_p(\Omega)$ to some admissible function ϕ, then $P_{pc}(\phi_k)$ converges to $P_{pc}(\phi)$ in $L_p(\Omega)$.
(vi) $|P_{pc}(\phi)|_{\mathtt{BV}}\leqslant\liminf_{k\to\infty}|P_{pc}(\phi_k)|_{\mathtt{BV}}$.
(vii) The L_4-norm is weakly lower semi-continuous with respect to L_4-convergence.

Proof. Let us prove item (i). We observe that $\mathcal{K}(\phi)-\mathcal{K}(\psi)=(\phi-\psi)(\phi+\psi-1)$. Hence, using Hölder inequality

$$\|\mathcal{K}(\phi)-\mathcal{K}(\psi)\|^2_{L_2(\Omega)}=\int_\Omega(\phi-\psi)^2(\phi+\psi-1)^2\,\mathrm{d}x\leqslant\|\phi-\psi\|^2_{L_4(\Omega)}\|\phi+\psi+1\|^2_{L_4(\Omega)}$$

and the continuity follows. The last assertion of item (i) follows from [15, lemma 2 (i)].

Assertion (ii) and (iv) follow immediately from the definition of $\mathcal{K}$ and P_{pc} respectively.

To prove assertion (iii), note that, since Ω is bounded, $\phi_k\rightharpoonup\bar{\phi}$ in $L_4(\Omega)$ implies that $\phi_k\rightharpoonup\bar{\phi}$ in $L_1(\Omega)$. Then, it follows from (i) that $\left\|\mathcal{K}(\bar{\phi})\right\|_{L_1(\Omega)}=0$.

Assertions (v) and (vi) follow from [12, lemma 9 items (ii) and (iii)] respectively. Assertion (vii) follows from [11, theorem 1.1, p 7] since $f(t)=t^4$ is a convex function. □

We are now ready to prove the main results of this section. We begin with an auxiliary lemma.

Lemma 3. *For any $\alpha > 0$, the functional $\widetilde{\mathcal{F}_\alpha}$ attains a minimizer on the set of admissible functions satisfying the constraint $\mathcal{K}(\phi) = 0$.*

Proof. It follows from assumption (A4) that $\widetilde{\mathcal{F}_\alpha}$ is proper. Let $\{\phi_k\}$ be a minimizing sequence of $\widetilde{\mathcal{F}_\alpha}$, i.e. a sequence of admissible functions satisfying $\widetilde{\mathcal{F}_\alpha}(\phi_k) \to \inf \widetilde{\mathcal{F}_\alpha} =: \Upsilon$, $k \to \infty$. Since $\widetilde{\mathcal{F}_\alpha}$ is proper, we have that $\Upsilon < \infty$. Therefore, $\{\widetilde{\mathcal{F}_\alpha}(\phi_k)\}$ has a convergent subsequence of real numbers (that we denote by simplicity with the same index). Moreover, from the definition of $\widetilde{\mathcal{F}_\alpha}$, we obtain that $\|\mathcal{K}(\phi_k)\|_{L_2(\Omega)} = 0$ and that $\{\|\phi_k\|_{L_4}\}$ is a bounded sequence of real numbers. Then, there exits a subsequence $\{\phi_{k_j}\}$ and $\bar{\phi} \in L_4(\Omega)$ such that $\phi_{k_j} \rightharpoonup \bar{\phi}$ in $L_4(\Omega)$. Moreover, from lemma 2(iv), we have that $\{|\phi_{k_j}|_{\mathtt{BV}}\}$ is a bounded sequence of real numbers. Then, by [15, lemma 1] we conclude that there exits of a subsequence $\{\phi_{k_{j_l}}\}$ and $\tilde{\phi} \in \mathtt{BV}(\Omega)$ such that $\{\phi_{k_{j_l}}\} \to \tilde{\phi}$ in $L_p(\Omega)$ for $1 \leqslant p < d/(d-1)$. It follows form the uniqueness of the weak limit that $\bar{\phi} = \tilde{\phi} \in L_4(\Omega) \cap \mathtt{BV}(\Omega)$. Moreover, from lemma 2 (iii), we conclude that $\mathcal{K}(\bar{\phi}) = 0$.

Finally, denoting by simplicity the above subsequence by $\{\phi_k\}$, it follows from assumption (A2) and lemma 2 (v)–(vii) that

$$\inf \widetilde{\mathcal{F}_\alpha} = \liminf_{k\to\infty} \widetilde{\mathcal{F}_\alpha}(\phi_k) = \liminf_{k\to\infty} \left\{\|F(P_{pc}(\phi_k)) - y^\delta\|_Y^2 + \alpha\mathcal{R}(\phi_k)\right\} \geqslant \widetilde{\mathcal{F}_\alpha}(\bar{\phi}),$$

proving that the admissible function $\bar{\phi}$ minimizes $\widetilde{\mathcal{F}_\alpha}$ satisfying $\mathcal{K}(\bar{\phi}) = 0$. □

Next we will prove the well-posedness of the constrained optimization problem (5).

Theorem 4. *For any $\alpha > 0$, the following assertions hold true:*

(i) Problem (5) has a solution on the set of admissible functions.
(ii) Let $\bar{\lambda}_\alpha$ be a vector supporting an exact penalty representation and $\mu_\alpha > \bar{\mu}_\alpha$ as in definition 2 (existence of $\bar{\lambda}_\alpha$, $\bar{\mu}_\alpha$ follow from theorem 1). Then, the augmented Lagrangian $\mathcal{L}_\alpha(\cdot; \bar{\lambda}_\alpha, \mu_\alpha)$ has a minimizer on the set of admissible solutions.
(iii) A solution of problem (5) can be obtained by solving the unconstrained optimization problem $\min_\phi \mathcal{L}_\alpha(\phi; \bar{\lambda}_\alpha, \mu_\alpha)$.

Proof. Assertion (i) follow immediately from lemma 3 and the definition of $\widetilde{\mathcal{F}_\alpha}$ (see definition 1). Assertion (ii) follows from lemma 3 and the identity in (10). Finally, assertion (iii) follows from theorem 1 and assertions (i) and (ii). □

In the next theorem we investigate convergence and stability of approximate solutions given by the primal solutions of the augmented Lagrangian approach. The proof follows standard arguments in the classical theory of Tikhonov regularization [18]. For the sake of completeness we chose to present the details.

Theorem 5 (Convergence). *Assume that we have exact data, i.e. $\delta = 0$ in (2). For every $\alpha > 0$ denote by ϕ_α a minimizer of $\mathcal{L}_\alpha(\cdot, \bar{\lambda}_\alpha, \mu_\alpha)$ on the set of admissible functions (the existence is guarantee in theorem 4). Then, for every sequence of positive numbers $\{\alpha_k\}$ converging to zero, the corresponding sequence $\{\phi_{\alpha_k}\}$ of minima of $\mathcal{L}_{\alpha_k}(\cdot, \bar{\lambda}_{\alpha_k}, \mu_{\alpha_k})$ has a subsequence (that we denote by the same index) $\{\phi_{\alpha_k}\}$ that is strongly convergent in $L_p(\Omega)$, for $1 \leqslant p < d/(d-1)$. The limit of $\{\phi_{\alpha_k}\}$ is an admissible solution. Moreover it is a solution of (4) with $y^\delta = y$.*

Proof. The existence of a minimum ϕ_{α_k} of $\mathcal{L}_{\alpha_k}(\phi;\bar{\lambda}_{\alpha_k},\mu_{\alpha_k})$ (for the corresponding generalized Lagrange multiplier supporting the exact penalty $(\bar{\lambda}_{\alpha_k},\mu_{\alpha_k})$) follows from theorem 4. Then, from assumption (A4) and the fact that ϕ_{α_k} is a minimum of $\mathcal{L}_{\alpha_k}(\phi;\bar{\lambda}_{\alpha_k},\mu_{\alpha_k})$, we obtain

$$\alpha_k\mathcal{R}(\phi_{\alpha_k}) \leqslant \mathcal{L}_{\alpha_k}(\phi_{\alpha_k};\bar{\lambda}_{\alpha_k},\mu_{\alpha_k}) \leqslant \mathcal{L}_{\alpha_k}(\hat{\phi};\bar{\lambda}_{\alpha_k},\mu_{\alpha_k}) = \alpha_k\mathcal{R}(\hat{\phi}). \tag{11}$$

Hence, $\{\|\phi_{\alpha_k}\|_{L_4}\}$ and $\{|P_{pc}(\phi_{\alpha_k})|_{\mathtt{BV}}\}$ are uniformly bounded sequence of real numbers. Consequently, by the same arguments given in the proof of lemma 3, we conclude that there exits a convergent subsequence (that we denote with the same index) $\{\phi_{\alpha_k}\}$ and an admissible limit function $\bar{\phi} \in \mathtt{BV}(\Omega)\cap L_4(\Omega)$ with $\phi_{\alpha_k} \to \bar{\phi}$ in $L_p(\Omega)$, for $1 \leqslant p < d/(d-1)$, and $\mathcal{K}(\bar{\phi}) = 0$.

Therefore, we have that form assumption (A2), lemma 2 items (v)–(vii) it follows that

$$\begin{aligned} 0 \leqslant \|F(P_{pc}(\bar{\phi})) - y\|_Y^2 &\leqslant \liminf_{k\to\infty}\{\|F(P_{pc}(\phi_{\alpha_k})) - y\|_Y^2 + \alpha_k\mathcal{R}(\phi_{\alpha_k})\} \\ &= \liminf_{k\to\infty}\mathcal{L}_{\alpha_k}(\phi_{\alpha_k}\bar{\lambda}_{\alpha_k},\mu_{\alpha_k}) \leqslant \liminf_{k\to\infty}\mathcal{L}_{\alpha_k}(\hat{\phi};\bar{\lambda}_{\alpha_k},\mu_{\alpha_k}) = 0. \end{aligned}$$

In the chain of inequalities, we further use the fact that $\mathcal{K}(\phi_{\alpha_k}) = 0$ in the third line, and equation (11) and finally the fact that $\alpha_k \to 0$ in the last one. Hence, we conclude that $y = F(P_{pc}(\bar{\phi}))$ as required. □

Next we show that the primal solutions of the augmented Lagrangian are stable w.r.t. noisy data.

Theorem 6 (Stability). *Let $\alpha = \alpha(\delta)$ be a positive function such that $\lim_{\delta\to 0}\alpha(\delta) = 0$ and $\lim_{\delta\to 0}\delta^2/\alpha(\delta) = 0$. Moreover, let $\{\delta_k\}$ a sequence of positive numbers converging to zero and $\{y^{\delta_k}\} \in Y$ be corresponding noisy data satisfying (2). Then, there exists a subsequence, denoted again by $\{\delta_k\}$, and a sequence $\{\alpha_k := \alpha(\delta_k)\}$ such that the corresponding minimizers ϕ_{α_k} of $\mathcal{L}_{\alpha_k}(\phi;\bar{\lambda}_{\alpha_k},\mu_{\alpha_k})$ converge in $L_p(\Omega)$, for $1 \leqslant p < d/(d-1)$ to a solution of (4) with $y^\delta = y$.*

Proof. Using assumption (A4) and that $\phi_{\alpha_k} \in \mathit{argmin}\,\mathcal{L}_{\alpha_k}(\phi;\bar{\lambda}_{\alpha_k},\mu_{\alpha_k})$, we obtain

$$\alpha_k\mathcal{R}(\phi_{\alpha_k}) \leqslant \mathcal{L}_{\alpha_k}(\phi_{\alpha_k};\bar{\lambda}_{\alpha_k},\mu_{\alpha_k}) \leqslant \mathcal{L}_{\alpha_k}(\hat{\phi};\bar{\lambda}_{\alpha_k},\mu_{\alpha_k}) \leqslant (\delta_k)^2 + \alpha_k\mathcal{R}(\hat{\phi}). \tag{12}$$

Now, from (12) and by the assumption on the sequence $\alpha_k(\delta_k)$, we have that $\{\mathcal{R}(\phi_{\alpha_k})\}$ is uniformly bounded. Then, as in the proof of theorem 5, we conclude that there exits a convergent subsequence (that we denote with the same index) $\{\phi_{\alpha_k}\}$ and a limit $\bar{\phi} \in \mathtt{BV}(\Omega)\cap L_4(\Omega)$ with $\phi_{\alpha_k} \to \bar{\phi}$ in $L_p(\Omega)$, $1 \leqslant p < d/(d-1)$ and $\mathcal{K}(\bar{\phi}) = 0$. Finally, the assertion follows by taking the limit in inequality (12), using assumption (A2), lemma 2 items (v)–(vii). □

We conclude this section relating the above results to the augmented Lagrangian approach proposed in [15], as well as, to the double-well potential approach commonly used by the community of phase field methods [37].

Remark 1. In [15] the constraint $K(\phi) = 0$ with $K(\phi) = \sqrt{|\phi||\phi-1|}$ is used (instead of $\mathcal{K}(\phi) = 0$ adopted here), and the admissible functions are chosen in $L_2(\Omega)\cap\mathtt{BV}(\Omega)$. It is possible to prove for K results analogous to those stated on lemma 2 (compare with [15, lemma 2]). Consequently, the convergence and stability results presented in this section can also be proved within the framework adopted in [15].

From the numerical point of view, the use of $\mathcal{K}$ instead of K is convenient. Since $\mathcal{K}$ is differentiable everywhere, the numerical implementation becomes more stable (see section 5.1).

Remark 2. In the phase field methods community (see, e.g. [37]) double-well potentials $\omega(\phi) := \phi^{2n}(\phi-1)^{2n}, n \in \mathbb{N}$ are commonly used in order to formulate a constraint ($\omega(\phi) = 0$) enforcing the level set function to be piecewise constant. Assuming that the level set functions ϕ are in $L_r(\Omega) \cap \mathtt{BV}(\Omega)$, with $r = 8n$, the convergence and stability results presented in this section can also be proved within this framework (i.e. an augmented Lagrangian approach with the double-well potentials as constraint can be characterized as a regularization method).

4. An iterative algorithm

The existence of an exact penalty representation justifies the implementation of a primal-dual algorithm to compute approximate solutions of the constrained optimization problem (5). In this section, we present the *inexact sub-gradient* (ISg) algorithm proposed in [6] and prove that this is a convergent method for solving the augmented Lagrangian PCLS approach.

The ISg algorithm generates a primal-dual sequence, with the advantage that it accepts an inexact solution of each sub-problem (this is in fact the actual situation in numerical implementations). In what follows the ISg algorithm is presented for the augmented Lagrangian PCLS approach.

For each $r \geqslant 0$, we define the set

$$A_r(\lambda,\mu) := \{\phi \in L_4(\Omega) : \mathcal{F}_\alpha(\phi) + \langle \lambda\,, \mathcal{K}(\phi)\rangle + \mu\|\mathcal{K}(\phi)\|_{L_2(\Omega)} \leqslant Q(\lambda,\mu) + r\}\,.$$

Choose $(\lambda_0,\mu_0) \in L_2(\Omega)\times\mathbb{R}_+$ such that $Q(\lambda_0,\mu_0) > -\infty$. Moreover, choose a prescribed tolerance $\epsilon^* > 0$, $\{\gamma_k\} \subset (0,\gamma)$ for some $\gamma > 0$, $\{r_k\} \subset \mathbb{R}_+$ with $r_k \to 0$ and also two scalars $\xi > \eta > 0$.

Step 0. Set $k := 0$.
Step 1. (Update the primal variable and test the stopping criteria)

(a) Find $\phi_k \in A_{r_k}(\lambda_k,\mu_k)$;
(b) if $\mathcal{K}(\phi_k) = 0$ and $r_k < \epsilon^*$, stop;
(c) if $\mathcal{K}(\phi_k) = 0$ and $r_k \geqslant \epsilon^*$, then $r_k := \frac{r_k}{2}$ and go to (a);
(d) if $\mathcal{K}(\phi_k) \neq 0$, go to Step 2.

Step 2. (Update the dual variables)

(a) Evaluate $\eta_k := \min\{\eta, \|\mathcal{K}(\phi_k)\|_{L_2}\}$ and $\xi_k := \max\{\xi, \|\mathcal{K}(\phi_k)\|_{L_2}\}$;
(b) Choose a step-size $s_k \in [\eta_k, \xi_k]$;
(c) Define $\lambda_{k+1} := \lambda_k + s_k\mathcal{K}(\phi_k)$ and $\mu_{k+1} := \mu_k + (\gamma_k+1)s_k\|\mathcal{K}(\phi_k)\|_{L_2}$;
(d) $k := k+1$, go to Step 1.

Note that the ISg algorithm has the general form of standard augmented Lagrangian methods: in Step 1 the primal variable ϕ_k is updated through the approximate solution of an unconstrained minimization problem with tolerance r_k; then in Step 2 the dual variables (λ_k,μ_k) are updated through an explicit formula. In the last case moving along a direction of dual ascent. The role of the parameters $\{\gamma_k\}$ is to ensure monotonic increase of the dual values. Furthermore, since $[\eta,\xi] \subset [\eta_k,\xi_k]$ for all k, a constant step-size for all iterations is admissible (see [6] for a discussion on other step-size rules).

The following theorem establishes primal convergence results of the ISg algorithm above (convergence of the dual sequence generated by the ISg algorithm is proven in [6, theorem

3.3]). The proof of theorem 7 follows the lines of the proof of [6, theorem 3.2], together with the existence of zero duality gap (guaranteed by theorem 1). In order to simplify the notation, we write $Q_k := Q(\lambda_k, \mu_k)$ for all k.

Theorem 7. *Consider the primal sequence $\{\phi_k\}$ generated by ISg algorithm. Take the parameter sequence $\{\gamma_k\}$ satisfying $\gamma_k \geqslant \bar{\gamma}$, for some $\bar{\gamma} > 0$. Then $\{\phi_k\}$ is bounded. Moreover, all its weak accumulation points are primal solutions, and $\{Q_k\}$ converges to the optimum value M_p.*

Sketch of the proof:

Let $\{\lambda_k, \mu_k\}$ be the dual sequence generated by the Step 2 of ISg algorithm. This sequence may be bounded or not. In either case, one follows the steps of the proof of [6, theorem 3.2] to conclude that $\|\mathcal{K}(\phi_k)\|_{L_2(\Omega)} \to 0$ (and consequently $\mathcal{K}(\phi_k) \rightharpoonup 0$ in $L_2(\Omega)$).

Therefore, due to the monotonicity of r_k, the weak duality property (that implies $Q_k \leqslant M_p$, $\forall k$) and the fact that $\phi_k \in A_{r_k}(\lambda_k, \mu_k)$, we conclude that $\{\mathcal{F}_\alpha(\phi_k)\}$ is uniformly bounded (see [6, lemma 3.4]). Consequently $\{\phi_k\}$ is bounded in $L_4(\Omega) \cap \mathtt{BV}(\Omega)$.

Arguing as in the proof of lemma 3, one proves the existence of a weak acumulation point $\widetilde{\phi} \in L_4(\Omega) \cap \mathtt{BV}(\Omega)$ of $\{\phi_k\}$. Since $\mathcal{F}_\alpha(\cdot)$ is weak lower semicontinuity, $\widetilde{\phi}$ minimizes $\mathcal{F}_\alpha(\cdot)$.

Now the existence of zero duality gap (item (ii) of theorem 1) together with the monotonicity of the sequence $\{Q_k\}$ (see [6, lemma 3.4]) imply the convergence of Q_k to the optimum value M_p. □

5. Numerical experiments

In this section, we implement the ISg numerical algorithm based on the level set approach derived in the previous sections, for the 2D diffuse optical tomography (DOT) benchmark problem. The DOT problem consists in the identification of the diffusion and absorption coefficients from a finite set of optical tomography data. For a detailed description of DOT see appendix A.

We conduct three types of experiments: (1) in section 5.2, we assume that the absorption coefficient c is known and focus on the identification of the diffusion coefficient a; (2) in section 5.3, we assume that a is known and consider the identification of the absorption coefficient c; (3) the simultaneous identification of both coefficients (a, c) is investigated in section 5.4.

The same setup of experiments was considered in [2]. This allow us to compare the results obtained using the approach proposed in this article, with the results obtained using the methodology derived in [2].

In all the numerical experiments presented below, we considered $\Omega = (0,1) \times (0,1)$. Furthermore, we have a vector of four ($\ell = 4$) measured Dirichlet data $\{y_m\}_{m=1}^4$, corresponding to four different Neumann boundary conditions $g_m \in L_2(\partial\Omega)$ (inputs). Each function g_m is supported at one of the four sides of $\partial\Omega$, e.g.

$$g_1(x_1, 0) = \begin{cases} 1, & x_1 \in (\frac{1}{4}, \frac{3}{4}) \\ 0, & x_1 \in (0, \frac{1}{4}) \cup (\frac{3}{4}, 1) \end{cases}$$

(g_1 is defined on $\Gamma_1 := \{(x_1, 0);\ x_1 \in (0,1)\}$). The other inputs $g_2(x_1, 1)$, $g_3(0, x_2)$ and $g_4(1, x_2)$ are defined analogously.

The exact data $y = F(u)$ is obtained by solving the elliptic boundary value problem in (A.1) (we use a finite element type method implemented in MATLAB). In order to avoid inverse crimes, the direct problem was solved at a uniform grid with 100 nodes at each boundary side.

However, in the numerical implementation of the level set method, all boundary value problems are solved at a uniform grid with 50 nodes at each boundary side.

5.1. Implementation issues

In general, the convergence of augmented Lagrangian algorithms is fast at the beginning and then it slows down when the solution is close to the true minimizer. In order to speed up the algorithm, in [32] the authors proposed a signed binary level set method where a modification of the level set function when computing $u = P_{pc}(\phi)$ is introduced. Instead of applying the level set functions ϕ directly, they suggest to replace this function by

$$\tilde{\phi}(x) = \begin{cases} 1\,, & \text{if } \phi(x) \geqslant 0.5 \\ 0\,, & \text{if } \phi(x) < 0.5 \end{cases}.$$

However, in the numerical implementation it is advisable to replace $\tilde{\phi}$ by a smoothed approximation. Following the ideas given in [32], we chose

$$\tilde{\phi}(x) = \frac{1}{2}\left(\frac{\phi(x) - 0.5}{\sqrt{(\phi(x) - 0.5)^2 + \epsilon_s}} + 1\right),$$

where ϵ_s is a small positive number. According to the suggestion given in [32], and also corroborated in some numerical experiments, it is convenient to start with a large value of ϵ_s and then decrease its value during the iterations.

Another advantage of this modification is that it helps to avoid local minima. Since, no restriction was imposed in the admissible set and by the lack of uniqueness in the case of finite measurements, a situation may occur in which a level set function with $\mathcal{K}(\phi) \neq 0$ produces an incorrect value of u but very similar data y. Equilibria of these kind of points should theoretically be avoided by the constraint $\mathcal{K}(\phi) = 0$; however, numerically, it may cause trouble. The suggested implementation, where ϕ is replaced by $\tilde{\phi}$, helps to considerably reduce this problem.

On the other hand, following the approach in [32], a solution of the minimization problem corresponding to Step 1(a) (see algorithm in section 4) was obtained by solving the optimality condition

$$\frac{\partial}{\partial \phi}\mathcal{L}_\alpha(\phi; \lambda, \mu) = 0\,. \tag{13}$$

In order to solve this optimality condition, an artificial time variable t is introduced and the PDE

$$\frac{\partial \phi}{\partial t} = \frac{\partial}{\partial \phi}\mathcal{L}_\alpha(\phi; \lambda, \mu)\,,$$

is solved until it reaches a steady solution (this strategy was used in [21] for solving optimality conditions related to optimization problems involving level set functions, and proved to be a stable one). This steady solution is also a solution of the optimality condition (13). We used the forward Euler method for calculating a steady solution of the above PDE.

It is worth mentioning that, in order to compute the optimality condition (13), the BV-seminorm should be approximated by the relaxed functional $B(w) = \int_\Omega \sqrt{|\nabla w|^2 + \epsilon_b}\,\mathrm{d}x$, where $\epsilon_b > 0$ ensures smoothness. The choice of $B(\cdot)$ is motivated by the fact that this relaxed functional has numerical advantages, such as differentiability when $\nabla w = 0$ (see [1] for details).

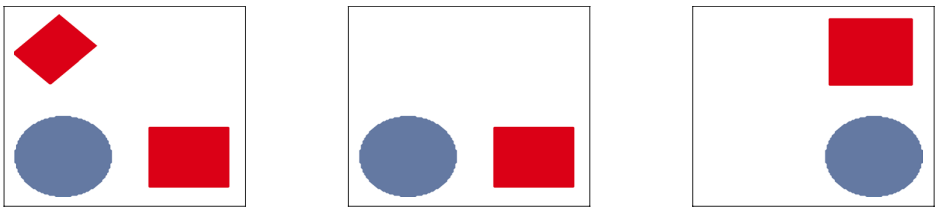

(a) (b) (c)

Figure 1. (a) Exact coefficients for the experiment presented in section 5.2 and the second experiment considered in section 5.3. (b) Exact coefficients for the first experiment in section 5.3. (c) Exact coefficients for all experiments in section 5.4.

In a similar way, the term corresponding to the L_2-norm is approximated by the functional $N(w) = \|\sqrt{\mathcal{K}(w)^2 + \epsilon_n}\|_{L_2}$, where $\epsilon_n > 0$. In both cases, it is desirable to start with a rather large value of ϵ_i, $i = b, n$, and then decrease its value during the iterations. Finally, we remark that here the election of $\mathcal{K}(t) = t(t-1)$ instead of $K(t) = \sqrt{|t||t-1|}$ (as in [15]) is useful, since the operator $\mathcal{K}$ is smooth everywhere whereas K is not even Lipschitz at $t = 0$ and $t = 1$.

5.2. Identification of the diffusion coefficient

In what follows, we consider the identification of the diffusion coefficient a assuming that the absorption coefficient c is known. The values for exact coefficients in all the experiments are

$$a^*(x) = \begin{cases} 10\,, & \text{inside blue inclusion} \\ 1\,, & \text{elsewhere} \end{cases}, \quad c^*(x) = \begin{cases} 10\,, & \text{inside red inclusion} \\ 1\,, & \text{elsewhere.} \end{cases}$$

as shown in figure 1. For this first example the exact solution is depicted in figure 1(a).

In all the experiments of this section, we chose 1 as the initial value for ϵ_i, $i = s, b, n$ and then decreased it by a factor of 0.9 in each iteration until the value reaches a lower bound equal to 10^{-6}. Additionally, when exact data were considered for the reconstruction (i.e. $\delta = 0$) we tested the iterative algorithm without the regularization term $|P_{pc}(\phi^j)|_{\mathtt{BV}}$, i.e. $\beta = 0$ (see [21, remark 5.1]). The regularization parameter α was chosen *a priori*: $\alpha = 10^{-3}$ (we experimented several different values for α, and this choice produced the best observed results). Moreover, we chose a constant step size $s_k = s = 10^{-2}$, a constant $\gamma_k = \gamma = 10^{-3}$, $r_k = 10^{-1} \times 0.99^k$, an Euler stepsize $\Delta = 5 \times 10^{-4}$ and prescribed tolerances $\tau = 10^{-3}$ and $\epsilon^* = 10^{-2}$. The penalty factor μ_0 and the generalized Lagrange multiplier λ_0 are initially set to zero. For details see algorithm in appendix B.

As initial guess, we chose $a_0 = P(\phi_0^a)$, where $\phi_0^a(x_1, x_2) = (x_1 - 0.5)^2 + (x_2 - 0.5)^2 + 0.5$. Other initial conditions were tested as well; the corresponding results obtained using distinct initial conditions were similar to the ones presented here. We point out that, the number of iterations necessary to achieve the same quality of reconstruction depends on choice of the initial guess. This situation is in agreement with the fact that the identification problem for the diffusion coefficient is known to be nonlinear and severely ill-posed [18, 24].

According to the obtained results the proposed method is able to identify the diffusion coefficient. The difference between the exact solution a^* and the approximated solution a_{300} is plotted in figure 2(a). The evolution of the iteration error $\|a^* - a_k\|_{L_1}$ is shown in figure 2(b). We can observe that the iteration stagnates after approximately 300 iterations.

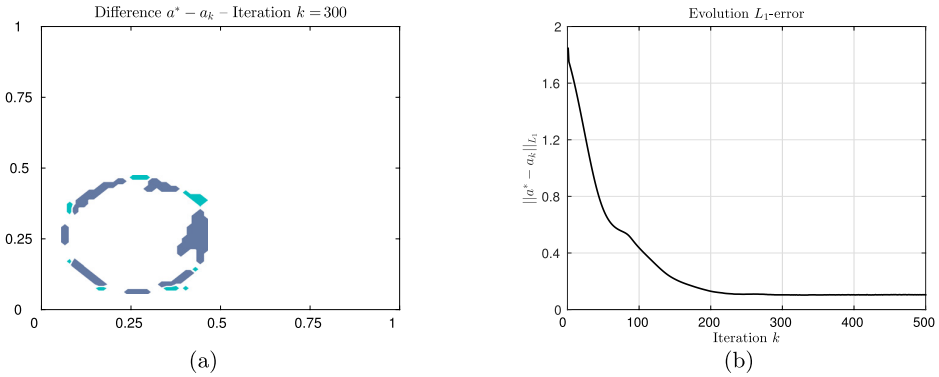

Figure 2. Experiment in section 5.2: identification of the diffusion coefficient a^* (absorption coefficient c^* is known). (a) Difference $a^*(x) - a_{300}(x)$ between the exact and computed coefficient. (b) Evolution of the iteration error $\|a^* - a_k\|_{L_1}$, $k = 0, \ldots, 500$.

It is worth mentioning that the same experiment was performed in [2] considering a SLS approach. In order to achieve an iteration error $\|a^* - a_k\|_{L_1} \approx 0.1$, circa 5000 iterations were needed using the SLS approach in [2]. On the other hand, with the current PCLS approach, approximately 300 iterations are needed in order to get a similar precision (see figure 2(b)). Therefore, the current approach significantly reduces the number of iterations compared with the methodology proposed in [2].

5.3. Identification of the absorption coefficient

In this subsection, we consider the identification of the absorption coefficient c. Two different experiments are performed. First, the identification of a coefficient c with connected support and then the identification of a coefficient c with non-connected support. The exact solutions of these experiments are shown in figures 1(a) and (b), respectively. In both cases the diffusion coefficient a is assume to be known.

Different initial level set functions ϕ_0^c and corresponding initial conditions c_0 were considered and, in all cases, the results were similar. In the experiments presented here we use $c_0 = P(\phi_0^c)$ where $\phi_0^c = \phi_0^a$ defined in section 5.2. The stepsize used in the Euler method is $\Delta = 2.5 \times 10^{-3}$. The remaining parameters are the same as in section 5.2 (see algorithm in appendix B).

We start with the identification of an absorption coefficient c with connected support. We can observe from figures 3(a) and (b) that the proposed augmented Lagrangian PCLS method is able to identify the shape of the absorption coefficient c. The corresponding difference between the exact solution c^* and the final iterate c_{300} is plotted in figure 3(a). The evolution of the iteration error $\|c^* - c_k\|_{L_1}$ is shown in figure 3(b).

Now, we turn to a more complex case: the identification of an absorption coefficient whose support is a non-connected proper subset of Ω. Once again the proposed methodology is able to identify the shape of the coefficient (see figures 4(a) and (b)). Despite that our initial guess was a level set function with connected support, the augmented Lagrangian PCLS method was able to identify both inclusions.

Let us note that the same experiment was performed in [2] considering a SLS approach. In that case, in order to achive an error $\|c^* - c_k\|_{L_1} \approx 0.2$, around 2250 iterations were needed.

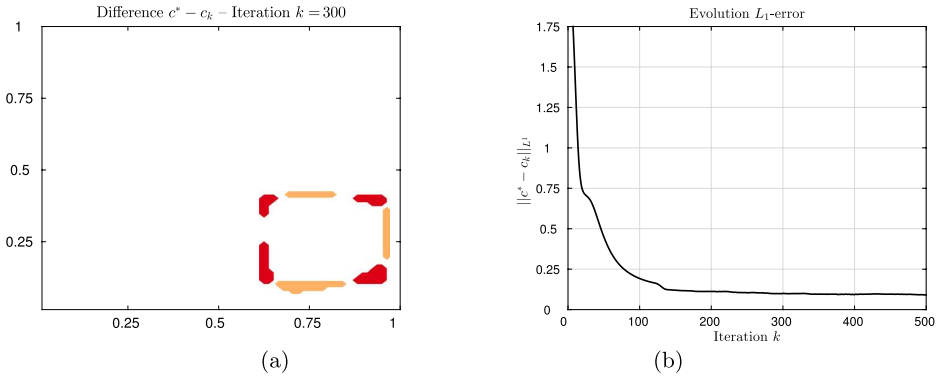

Figure 3. Experiment in section 5.3: identification of the absorption coefficient c^* with connected support (diffusion coefficient a^* is known). (a) Difference $c^*(x) - c_{300}(x)$ between the exact and computed coefficient. (b) Evolution of the iteration error $\|c^* - c_k\|_{L_1}$, $k = 0, \ldots, 500$.

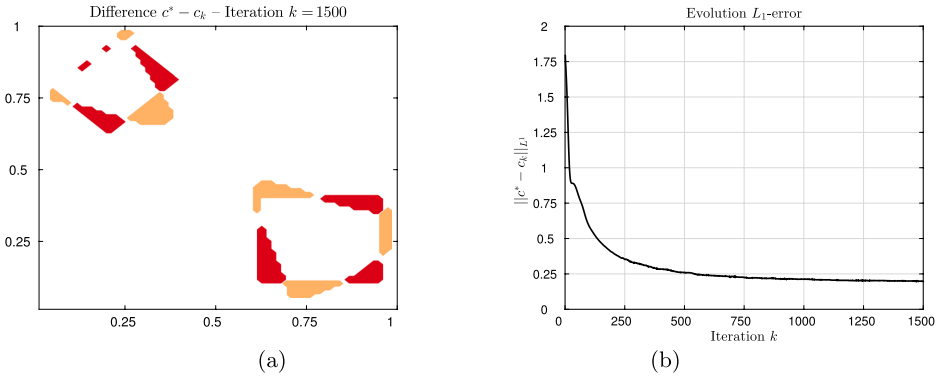

Figure 4. Experiment is section 5.3: identification of the absorption coefficient c^* with non-connected support (diffusion coefficient a^* is known). (a) Difference $c^*(x) - c_{1500}(x)$ between the exact and approximated solutions. (b) Evolution of the iteration error $\|c^* - c_k\|_{L_1}$, $k = 0, \ldots, 1500$.

On the other hand, with the current PCLS approach we needed approximately 1250 iterations (see figure 4(b)). Therefore, once again the proposed method reduces the number of iterations.

5.4. Identification of the diffusion and absorption coefficient

In this last set of experiments, we focus on the simultaneous identification of the pair of coefficient (a, c) in figure 1(c). First, we concentrate on the identification of both coefficient using exact data. Then, in a second experiment we consider the case of noisy data.

Motivated by the fact that the identification of coefficient c is a mildly ill-posed problem whereas the reconstruction of coefficient a is a severely ill-posed problem, a split strategy was proposed in [2]. It consists in freezing $a = a_0$ and first iterating with respect to c up to the iteration stagnate (this is an indicator that the iteration error $\|c_{k_1} - c^*\|_{L_1}$ is small). Then, keep $c = c_{k_1}$ and start iterating with respect to a until stagnation of the iteration. Finally, once

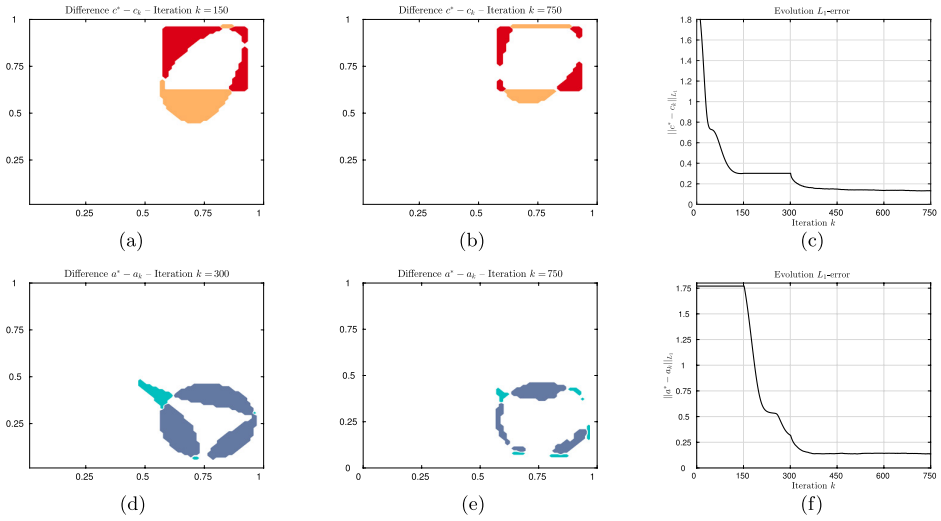

Figure 5. Experiment in section 5.4: simultaneous identification of both coefficients using exact data y. (a)–(c) Identification of the absorption coefficient c^*. (a) Difference $c^*(x) - c_{150}(x)$, end of the first stage of the split algorithm ($k_1 = 150$). (b) Difference $c^*(x) - c_{750}(x)$. (c) Evolution of the error $\|c^* - c_k\|_{L_1}$, $k = 0, \ldots, 750$. (d)–(f) Identification of the diffusion coefficient a^*. (d) Difference $a^*(x) - a_{300}(x)$, end of the second stage of the split algorithm ($k_2 = 300$). (e) Difference $a^*(x) - a_{750}(x)$. (f) Evolution of the error $\|a^* - a_k\|_{L_1}$, $k = 0, \ldots, 750$.

adequate approximations for both parameters are available, start iterating with respect to both coefficients.

This 3-stage numerical strategy allows the computation of accurate approximations for both coefficients. Moreover, it contributes to the reduction of the computational effort. Here, this strategy is coupled to the augmented Lagrangian PCLS method.

It is worth noticing that the calculation of the optimal transition indexes k_1, k_2 between the three stages could be a difficult task. However, taking into account the previous experiments in sections 5.2 and 5.3, we concluded that (in both cases) circa 150 iterations are enough to compute acceptable approximations of a^* and c^*. Therefore, in the next examples we take $k_1 = k_2 = 150$.

5.4.1. Exact data. We consider the identification problem with exact solution shown in figure 1(c). The stepsizes used in the Euler method are $\Delta_a = 2.5 \times 10^{-4}$ for the coefficient a and $\Delta_c = 5 \times 10^{-4}$ for the coefficient c. The remaining parameters and initial guess ϕ_0^a and ϕ_0^c are the same as the ones described in sections 5.2 and 5.3 (see algorithm in appendix B).

The results of the first stage are plotted in figures 5(a) and (c). The difference between the exact coefficient c^* and the approximated solution c_{k_1} is shown in figure 5(a) while the evolution of the iteration error corresponding to the first $k_1 = 150$ steps can be observed in figure 5(c). Note that $\|a_k - a^*\|_{L_1}$ remains constant for $k = 0, \ldots, k_1$, see figure 5(f).

Once the first stage is concluded, we freeze $c_k = c_{k_1}$ and iterate only with respect to a_k. This characterizes the second stage of the method. The corresponding evolution of the iteration error can be observed in figures 5(c) and (f). Note that now $\|a_k - a^*\|_{L_1}$ starts to decrease

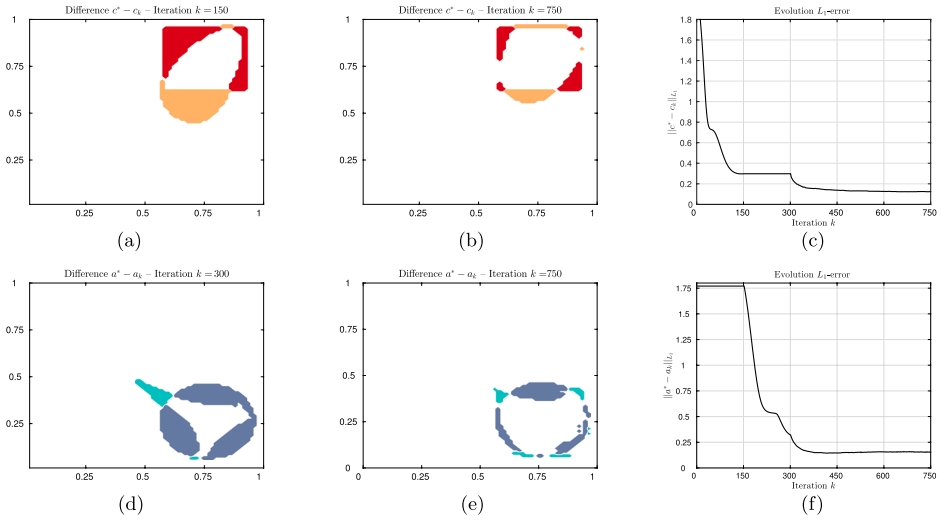

Figure 6. Experiment in section 5.4: simultaneous identification of both coefficients using noisy data y^δ. (a)–(c) Identification of the absorption coefficient c^*. (a) Difference $c^*(x) - c_{150}(x)$, end of the first stage of the split algorithm ($k_1 = 150$). (b) Difference $c^*(x) - c_{750}(x)$. (c) Evolution of the error $\|c^* - c_k\|_{L_1}$, $k = 0, \ldots, 750$. (d)–(f) Identification of the diffusion coefficient a^*. (d) Difference $a^*(x) - a_{300}(x)$, end of the second stage of the split algorithm ($k_2 = 300$). (e) Difference $a^*(x) - a_{750}(x)$. (f) Evolution of the error $\|a^* - a_k\|_{L_1}$, $k = 0, \ldots, 750$.

significantly, while $\|c_k - c^*\|_{L_1}$ remains constant for $k = k_1, \ldots, k_2 = 300$. The difference $a_{k_2} - a^*$ is plotted in figure 5(d).

After the termination of the second iteration stage, the pair (a_{k_2}, c_{k_2}) is a good approximation of (a^*, c^*) (see figures 5(a) and (d)). As a matter of fact, this approximation is so good that proceeding with the iteration simultaneously with respect to both coefficients, the iteration errors $\|a_k - a^*\|_{L_1}$ and $\|c_k - c^*\|_{L_1}$ are decreasing. The final difference between the exact and the approximated coefficients are plotted in figures 5(b) and (e).

Let us remark that same experiment, with an identical set-up, was performed in [2] considering a SLS approach. Again, to achieve the same error, the proposed PCLS methodology requires close to half of the iterations needed using the SLS approach.

5.4.2. Noisy data. We consider the identification problem with exact solution shown in figure 1(c). This time we consider noisy data y_m^δ obtained by adding to the exact data $y_m = F_m(u)$ random generated noise of 5%.

For this experiment with noisy data, the augmented Lagragian PCLS method was tested with the BV regularization term taking $\beta = 10^{-3}$. The initial guesses ϕ_0^a and ϕ_0^c and the remaining parameters are the same as the ones used in the above experiment with exact data.

We applied again the 3-stage strategy described before. The results of the first stage are plotted in figures 6(a) and (c), where the difference between the exact solution c^* and the approximated solution c_{k_1} and the evolution of the iteration error corresponding to the first $k_1 = 150$ steps can be observed, respectively. Note that $\|a_k - a^*\|_{L_1}$ remains constant for $k = 0, \ldots, k_1$ while $\|c_k - c^*\|_{L_1}$ starts to decrease.

After the first iteration stage, we freeze $c_k = c_{k_1}$ and iterate only with respect to a_k. The evolution of the iteration error can be observed again in figure 6(f) where one can see that $\|a_k - a^*\|_{L_1}$ starts to decrease. The difference between the exact solution a^* and the approximated solution a_{k_2} is plotted in figure 6(d).

Finally, we proceed to iterate simultaneously with respect to both coefficients. The iteration errors $\|c_k - c^*\|_{L_1}$ and $\|a_k - a^*\|_{L_1}$ are decreasing as can be seen in figures 6(c) and (f), respectively. The difference between the exact and the approximated coefficients, after 750 iterations are plotted in figures 6(b) and (e).

6. Conclusions

We proposed and analysed a method for solving ill-posed nonlinear operator equations in L_p-spaces. The goal is to identify the level sets of a parameter function, which is known to be piecewise constant and takes known values.

The original parameter identification problem was rewritten in the form of a constrained optimization problem, which turns out to be non-convex. Therefore, classical Lagrange multiplier methods cannot be applied. Following [15], we used an augmented Lagrangian method known in the literature as sharp Lagrangian.

We proved for our method similar results to those obtained in [15]; namely, the existence of zero duality gaps and the existence of generalized Lagrangian multipliers. Moreover, we extended the analysis initiated in [15], proving convergence and stability of our novel parameter identification method (i.e. the solution method is a regularization method in the sense of [18]).

A convergent primal-dual iterative method was proposed to compute approximate solutions, and was tested for a 2D diffuse optical tomography benchmark problem, with consists in the simultaneous identification of the diffusion and absorption coefficients from boundary measurements of the solution of an elliptic equation. Several experiments were conducted in order to compare the performance of our algorithm with the standard level set SLS method proposed in [2].

The numerical results indicate that the proposed method is able to identify the absorption and diffusion coefficients with the same quality than the SLS method employed in [2]. Moreover, in all the conducted experiments, our iterative method requires a smaller number of iterations when compared with the iterative method in [2].

Acknowledgments

JPA acknowledges support from SECyT-UNC grant 30820150100062CB and CONICET grant PIP 112201-501005-00CO. ADC acknowledges support from FAPERGS PPP-ARD, grant 16/2551-0000211-8, and CNPq, grant 301499/2017-9. AL acknowledges support from CNPq, grant 311087/2017-5, and from the Alexander von Humboldt foundation AvH.

Appendix A. Diffuse optical tomography

Diffusive optical tomography (DOT) is a non-invasive image methodology that uses light in the near-infrared spectral region to measure the optical properties of a physical body. DOT

has demonstrated to be a powerful technique to obtain relevant physiological information of tissues in a non-invasive manner [4].

Denoting the photon density by w, the following model is used for representing the underlying physical phenomena (see, e.g. [4])

$$-\nabla \cdot (a(x)\nabla w) + c(x)w = 0 \text{ in } \Omega, \qquad a(x)\nabla w \cdot \nu = g \quad \text{on } \partial\Omega, \tag{A.1}$$

where $\Omega \subset \mathbb{R}^d$ is bounded domain with Lipschitz boundary, $a(x)$ is the diffusion coefficient, $c(x)$ represents the absorption coefficient and $g \in H^{-1/2}(\partial\Omega)$ is the Neumann boundary data. Such boundary condition can be interpreted as the exitance on $\partial\Omega$.

Since the optical properties within tissue are determined by the values of the diffusion and absorption coefficients, the problem of interest in DOT is the simultaneous identification of both coefficients (a, c) from measurements of near-infrared diffusive light along the tissue boundary.

Let us state the inverse problem for DOT in terms of the notation used in this manuscript. For each input $g \in H^{-1/2}(\partial\Omega)$ in (A.1), we define the *parameter-to-measurement* forward map

$$F_g := F : D(F) \to H^{1/2}(\partial\Omega), \qquad F_g(a, c) = y := w|_{\partial\Omega}, \tag{A.2}$$

where $w = w(g)$ is the unique solution of (A.1), given the boundary data g and the pair (a, c) in the parameter space $D(F_g) := \{(a, c) \in L_1(\Omega) \times L_1(\Omega) : 0 < m_1 \leqslant a(x), c(x) \leqslant m_2\}$. Here m_1 and m_2 are given positive real numbers.

It is a well established fact [23] that the full Neumann-to-Dirichlet map is needed to prove unique identification of the parameters (a, c) in (A.1). Here, as in real life applications, we assume that only a finite number $\ell \in \mathbb{N}$ of experiments is available. The inverse problem under consideration consists in the simultaneous reconstruction of (a, c) in (A.1) from a finite number of inputs $g_m = a\frac{\partial w_m}{\partial \nu}|_{\partial\Omega}$ and corresponding (measured) data $y_m = w_m|_{\partial\Omega}$, i.e.

$$F_{g_m}(a, c) = y_m, \qquad m = 1, \ldots, \ell,$$

where F_{g_m} is defined as in (A.2), for each $m \in \{1, \ldots, \ell\}$.

The next result guarantees that the parameter-to-measurement F_g satisfies the assumptions (A2). For a proof we refer the reader to [2, theorem 2.5].

Proposition A.1. *For each $g \in H^{-1/2}(\partial\Omega)$ the corresponding operator $F_g : D(F_g) \longrightarrow H^{-1/2}(\partial\Omega)$ is continuous w.r.t. the $L_1(\Omega) \times L_1(\Omega)$-topology.*

In terms of the notation used in section 1, we shall consider $u = (a, c)$ and $X = L_1(\Omega) \times L_1(\Omega)$. As a consequence, two level set functions (ϕ^a, ϕ^c) are needed: one to parameterize the diffusion coefficient $a = P_{pc}(\phi^a)$, and another one to parameterize the absorption coefficient $c = P_{pc}(\phi^c)$.

The constrained optimization problem (5) becomes

$$\begin{cases} \min\limits_{\phi^a, \phi^c} \mathcal{F}_\alpha(\phi^a, \phi^c) := \|F_g(P_{pc}(\phi^a), P_{pc}(\phi^c)) - y^\delta\|_Y^2 + \alpha\big[\mathcal{R}(\phi^a) + \mathcal{R}(\phi^c)\big] \\ \text{s.t. } \mathcal{K}(\phi^a) = 0 \quad \text{and} \quad \mathcal{K}(\phi^c) = 0. \end{cases}$$

The corresponding augmented Lagrangian functional reads

$$\begin{aligned} \mathcal{L}_\alpha(\phi^a, \phi^c;\ \lambda^a, \mu^a, \lambda^c, \mu^c) := \mathcal{F}_\alpha(\phi^a, \phi^c) + \langle \lambda^a, \mathcal{K}(\phi^a)\rangle_{L_2(\Omega)} + \mu^a\|\mathcal{K}(\phi^a)\|_{L_2(\Omega)} \\ + \langle \lambda^c, \mathcal{K}(\phi^c)\rangle_{L_2(\Omega)} + \mu^c\|\mathcal{K}(\phi^c)\|_{L_2(\Omega)}. \end{aligned}$$

Table B1. Algorithm used in the numerical experiments.

Take an initial condition ϕ_0 and set $\lambda_0 = 0 \in L_2(\Omega)$ and $\mu_0 = 0 \in \mathbb{R}$.

Fix $s_k = s > 0$, $\gamma_k = \gamma > 0$, $\{r_k\} \subset \mathbb{R}_+$ with $r_k \to 0$, $\tau > 0$, $\epsilon^* > 0$.

Let $k := 0$

1. Update primal variable ϕ_k:

1.1 Inner iteration : choose $\Delta > 0$, set $\bar{\phi}_0 = \phi_k$ and $n = 0$;

(i) Evaluate the residual $[\xi_{n,m}]_{m=1}^{\ell} := [F_{g_m}(P_{pc}(\bar{\phi}_n)) - y_m^{\delta}]_{m=1}^{\ell}$;

(ii) Evaluate $\left[\left(\frac{\partial F_{g_m}(P_{pc}(\bar{\phi}_n))}{\partial \phi}\right)^* \xi_{n,m}\right]_{m=1}^{\ell}$;

(iii) Evaluate $\frac{\partial \mathcal{R}(\bar{\phi}_n)}{\partial \phi}$;

(iv) If $\|\frac{\partial}{\partial \phi}\mathcal{L}_\alpha(\bar{\phi}_n; \lambda_k, \mu_k)\| \geqslant \sqrt{10^{-1} r_k}$ then

$\bar{\phi}_{n+1} = \bar{\phi}_n - \Delta \frac{\partial}{\partial \phi}\mathcal{L}_\alpha(\bar{\phi}_n; \lambda_k, \mu_k)$;

n := n + 1; go to (i);

else

n^*: $= n$;

1.2 Stopping criteria:

if $\|\mathcal{K}(\bar{\phi}_{n^*})\| < \tau$ then

if $r_k < \epsilon^*$ then

stop;

else

$r_k := \frac{r_k}{2}$ and go to **1.1**;

else

$\phi_{k+1} := \bar{\phi}_{n^*}$;

2 Update dual variables:

$\lambda_{k+1} := \lambda_k + s\mathcal{K}(\phi_{k+1})$, and $\mu_{k+1} := \mu_k + (\gamma + 1)s\|\mathcal{K}(\phi_{k+1})\|$

Define $k := k + 1$ and go to **1**.

Note that the admissible pairs (ϕ^a, ϕ^c) as well as all other functions/functionals in definition 1 can be adapted accordingly to the above cartesian product setup. A careful inspection of sections 3 and 4 shows that the results in lemma 3 and theorems 1 and 4–7 remain valid in the above framework. Consequently, the method discussed in this article can be used to simultaneously identify the coefficients (a, c).

Appendix B. Algorithm used in the numerical experiments

In this appendix we describe in detail the algorithm used in the numerical experiments presented in section 5 (see table B1). We remark that for the identification of the diffusion coefficient a (DOT model in sections 5.2 and 5.4) and for the identification of the absorption coefficient c (DOT model in sections 5.3 and 5.4), item (ii) in table B1 is computed using the formulas

$$\left(\frac{\partial F_{g_m}(P_{pc}(\phi_n^a))}{\partial \phi_n^a}\right)^* \xi_{n,m} = -\nabla w_{n,m} \cdot \nabla v_{n,m}, \qquad \left(\frac{\partial F_{g_m}(P_{pc}(\phi_n^c))}{\partial \phi_n^c}\right)^* \xi_{n,m} = -w_{n,m}\, v_{n,m},$$

respectively. Here $w_{n,m} \in H^1(\Omega)$ is the unique solution of problem (A.1) and $v_{n,m} \in H^1(\Omega)$ is the unique solution of the boundary value problem

$$-\nabla \cdot (a_n(x)\nabla v) + c_n(x)v = 0 \text{ in } \Omega, \qquad a_n(x)\nabla v \cdot \nu = \xi_{n,m} \quad \text{on } \partial\Omega.$$

ORCID iDs

A De Cezaro https://orcid.org/0000-0001-8431-9120

References

[1] Acar R and Vogel C 1994 Analysis of bounded variation penalty methods for ill-posed problems *Inverse Problems* **10** 1217–29
[2] Agnelli J, De Cezaro A, Leitão A and Marques Alves M 2017 On the identification of piecewise constant coefficients in optical diffusion tomography by level set *ESAIM: COCV* **23** 663–83
[3] Álvarez D, Dorn O, Irishina N and Moscoso M 2009 Crack reconstruction using a level-set strategy *J. Comput. Phys.* **228** 5710–21
[4] Arridge S R 1999 Optical tomography in medical imaging *Inverse Problems* **15** R41–93
[5] Burachik R S, Iusem A N and Melo J G 2010 Duality and exact penalization for general augmented Lagrangians *J. Optim. Theory Appl.* **147** 125–40
[6] Burachik R S, Iusem A N and Melo J G 2013 An inexact modified subgradient algorithm for primal-dual problems via augmented lagrangians *J Optim. Theory Appl.* **157** 108–31
[7] Burger M 2001 A level set method for inverse problems *Inverse Problems* **17** 1327–55
[8] Burger M and Osher S 2005 A survey on level set methods for inverse problems and optimal design *Eur. J. Appl. Math.* **16** 263–301
[9] Chan T F and Tai X C 2003 Level set and total variation regularization for elliptic inverse problems with discontinuous coefficients *J. Comput. Phys.* **193** 40–66
[10] Chung E T, Chan T F and Tai X C 2005 Electrical impedance tomography using level set representation and total variational regularization *J. Comput. Phys.* **205** 357–72
[11] Dacorogna B 1982 *Weak Continuity and Weak Lower Continuity of Nonlinear Functionals* (*Lecture Notes in Mathematics* vol 922) (New York: Springer)
[12] De Cezaro A and Leitão A 2012 Level-set approaches of L_2-type for recovering shape and contrast in ill-posed problems *Inverse Problems Sci. Eng.* **20** 571–87
[13] De Cezaro A, Leitão A and Tai X C 2009 On level-set type methods for recovering piecewise constant solutions of ill-posed problems *Scale Space and Variational Methods in Computer Vision* (*Lecture Notes in Computer Science* vol 5667) ed X-C Tai *et al* (Berlin: Springer) pp 50–62
[14] De Cezaro A, Leitão A and Tai X C 2009 On multiple level-set regularization methods for inverse problems *Inverse Problems* **25** 035004
[15] De Cezaro A, Leitão A and Tai X C 2013 On piecewise constant level-set (pcls) methods for the identification of discontinuous parameters in ill-posed problems *Inverse Problems* **29** 015003
[16] Dorn O and Lesselier D 2006 Level set methods for inverse scattering *Inverse Problems* **22** R67–131
[17] Dorn O and Lesselier D 2015 Level set methods for structural inversion and image reconstruction *Handbook of Mathematical Methods in Imaging* ed O Scherzer (New York: Springer) pp 471–532
[18] Engl H W, Hanke M and Neubauer A 1996 *Regularization of Inverse Problems* (*Mathematics and its Applications* vol 375) (Dordrecht: Kluwer)
[19] Evans L C and Gariepy R F 1992 *Measure Theory and Fine Properties of Functions* (*Studies in Advanced Mathematics*) (Boca Raton, FL: CRC Press)
[20] Frick K and Scherzer O 2010 Regularization of ill-posed linear equations by the non-stationary augmented Lagrangian method *J. Integral Equations Appl.* **22** 217–57
[21] Frühauf F, Scherzer O and Leitão A 2005 Analysis of regularization methods for the solution of ill-posed problems involving discontinuous operators *SIAM J. Numer. Anal.* **43** 767–86
[22] Glowinski R and Le Tallec P 1989 *Augmented Lagrangian and Operator-Splitting Methods in Nonlinear Mechanics* (*SIAM Studies in Applied Mathematics* vol 9) (Philadelphia, PA: SIAM)
[23] Harrach B 2009 On uniqueness in diffuse optical tomography *Inverse Problems* **25** 055010
[24] Isakov V 2006 *Inverse Problems for Partial Differential Equations* (*Applied Mathematical Sciences* vol 127) 2nd edn (New York: Springer)
[25] Ito K and Kunisch K 2008 *Lagrange Multiplier Approach to Variational Problems and Applications* (*Advances in Design and Control* vol 15) (Philadelphia, PA: SIAM)

[26] Ito K, Kunisch K and Li Z 2001 Level-set function approach to an inverse interface problem *Inverse Problems* **17** 1225
[27] Koko J and Jehan-Besson S 2010 An augmented Lagrangian method for $tv_g = l^1$-norm minimization *J. Math. Imaging Vis.* **38** 182–96
[28] Leitão A, Markowich P A and Zubelli J P 2006 On inverse doping profile problems for the stationary voltagecurrent map *Inverse Problems* **22** 1071
[29] Leitão A and Marques Alves M 2007 On level set type methods for elliptic cauchy problems *Inverse Problems* **23** 2207
[30] Leitão A and Scherzer O 2003 On the relation between constraint regularization, level sets, and shape optimization *Inverse Problems* **19** L1–11
[31] Litman A, Lesselier D and Santosa F 1998 Reconstruction of a two-dimensional binary obstacle by controlled evolution of a level-set *Inverse Problems* **14** 685–706
[32] Nielsen L K, Tai X C, Aanonsen S I and Espedal M 2007 A binary level set model for elliptic inverse problems with discontinuous coefficients *Int. J. Numer. Anal. Model.* **4** 74–99
[33] Rockafellar R T and Wets R J-B 1998 *Variational Analysis* (*Grundlehren der Mathematischen Wissenschaften (Fundamental Principles of Mathematical Sciences)* vol 317) (Berlin: Springer)
[34] Santosa F 1995/96 A level-set approach for inverse problems involving obstacles *ESAIM Contrôle Optim. Calc. Var.* **1** 17–33
[35] Tai X C and Chan T F 2004 A survey on multiple level set methods with applications for identifying piecewise constant functions *Int. J. Numer. Anal. Model.* **1** 25–47
[36] Wu C, Zhang J and Tai X C 2011 Augmented Lagrangian method for total variation restoration with non-quadratic fidelity *Inverse Problems Imaging* **5** 237–61
[37] Zhu S and Liu C 2011 A semi-implicit binary level set method for source reconstruction problems *Int. J. Numer. Anal. Model.* **8** 410–26